Green Chemistry

PAPER

View Article Online
View Journal

Cite this: DOI: 10.1039/d5gc05638a

Expanding the product spectrum in mixed-culture fermentation of organic solid waste through operational control

Hanna Prusak, [a] Natalia Gutowska, [a] Emilie Alaux, [b] Mateusz Szczygiełda, [c] Nay Yee Wint,[a] Diana Z. Sousa,[b] Mateusz Łężyk [a] and Piotr Oleskowicz-Popiel *[a]

Received 23rd October 2025,
Accepted 7th January 2026

DOI: 10.1039/d5gc05638a

rsc.li/greenchem

The microbial synthesis of value-added biochemicals offers an attractive, sustainable alternative to conventional production methods. This study investigates mixed-culture fermentation (MCF) of the organic fraction of municipal solid waste (OFMSW) under varying operational conditions (temperature, pH, and hydraulic retention time (HRT)). The aim was to improve the production of selected carboxylates, including succinate and caproate. Furthermore, by assessing the metabolic roles of identified taxa and their responses to different process conditions, potential functional links between community composition and product formation were proposed. Under mesophilic conditions (37 °C), shifts in pH and HRT strongly influenced product distribution: succinate and propionate predominated at shorter HRTs, whereas caproate production prevailed at pH 6.5–7.0, 37 °C, and HRT of 5 days, reaching 515 mM C. Thermophilic (50 °C) operation favored the synthesis of ethanol, lactate, and butyrate. These findings demonstrate how operational strategies and microbial community dynamics can be leveraged to tailor product spectra in MCF.

Green foundation

1. The pressing need to defossilise the chemical industry is driving research on the sustainable production of bio-based chemicals like succinic or caproic acid. Our work provides insights into mixed culture fermentation of waste-derived feedstock to the desired bio-chemicals.
2. This study assessed the optimal conditions of not-yet-well-explored succinate production by mixed cultures, obtaining the desired bio-product from a waste-biomass at an average 35% specificity, and productivity of 0.14 g L^{-1} h^{-1}. Moreover, we created optimal conditions for an efficient caproate synthesis with no external electron donor (average 34% specificity).
3. To make the process both, greener and industrially relevant, several aspects would be influential to explore. These include a deeper investigation into the interactions among mixed culture members and thermodynamic constraints. Such research could enhance understanding, enabling better control and optimization of the process, with the potential to achieve higher titers and improved selectivity.

Introduction

Waste not, want not: biochemicals to the rescue

Due to the scarcity and environmental impact associated with the use of fossil resources – which still form the basis for chemicals and energy production – there has been a noticeable shift in legislation, research, and commercialization trends toward bio-based products and renewable energy. While composting, incineration, and anaerobic digestion are established methods for organic waste valorization, they primarily aim at waste treatment or energy recovery.[1–3] In contrast, sustainable biochemical production focuses on converting waste into value-added chemical intermediates, offering higher resource recovery potential.[1]

The handling of municipal solid waste (MSW), generated by households and public institutions, remains a significant environmental challenge.[4] About 15.6–71.5% of MSW consists of organic material that can be further utilized for carbon recycling.[5] According to EUROSTAT, in 2022, the average amount of MSW generated in the European Union was 513 kg per capita, of which 48% was recycled.[3] In 2021, MSW landfills accounted for approximately one-third of human-related methane emissions in the United States,[6] underscoring their substantial contribution to greenhouse gas emissions. The

[a]Water Supply and Bioeconomy Division, Faculty of Environmental Engineering and Energy, Poznan University of Technology, Berdychowo 4, 60-965 Poznan, Poland. E-mail: piotr.oleskowicz-popiel@put.poznan.pl
[b]Laboratory of Microbiology, Wageningen University and Research, Stippeneng 4, 6708 WE Wageningen, The Netherlands
[c]Institute of Chemical Technology and Engineering, Faculty of Chemical Technology, Poznan University of Technology, Berdychowo 4, 60-965 Poznan, Poland

organic fraction of municipal solid waste (OFMSW) is commonly applied for biogas production through anaerobic digestion, or for hydrochar production through hydrothermal carbonization.[5,7] In recent years, however, biochemical production has emerged as an attractive alternative for OFMSW valorization, enabling the synthesis of value-added metabolites such as organic acids, alcohols, and biopolymers.[5,7–10] These fermentation-derived compounds serve as important platform chemicals for bio-based industries and can be integrated into biorefinery frameworks guided by the principles of the circular economy.

Unleashing the potential of mixed cultures in waste conversion

Biochemical production through MCF represents a promising approach for advancing sustainable waste management. One of its key advantages is the ability to process complex, waste-derived organic feedstocks or waste gases without the need for strict sterility.[11–13] This eliminates one of the most energy-intensive requirements of pure-culture fermentation, thereby reducing overall energy demand and considerably lowering the environmental footprint of the bioprocess. Moreover, division of labour and metabolic specialization among community members not only expand substrate utilization capacity but also relieve thermodynamic bottlenecks in metabolic pathways through synergistic interactions among microbial species.[14,15] As a result, the production of the desired intermediates and products may proceed more rapidly.[14–16] Although specialized functions may be disrupted by fluctuations in environmental conditions, broad functions such as carbon metabolism and biomass production tend to be more resilient in mixed cultures, enhancing their overall adaptability.[15,17]

Learning to control microbial communities through changes in environmental conditions is particularly appealing, as it offers the potential to direct the same consortium toward the production of different chemicals. A deeper understanding of how operational parameters – specifically pH, temperature, and hydraulic retention time (HRT) – affect the microbiome and its metabolism is therefore essential. In response to changing environmental conditions, members of a mixed culture dynamically adjust their metabolic activities through collective trade-offs and synergistic interactions within the communities.[18] This, in turn, results in predictable shifts in metabolite composition.[18] Such metabolism-driven transitions have been documented under various operational conditions. For example, Quintela *et al.* demonstrated a substantial pH influence in MCF.[19] Increasing pH from 4.5 to 6.0 led to a 10.7-fold increase in butyrate titers, and the emergence of caproate production, rising from non-detected to 0.97 ± 0.05 g L^{-1} day^{-1}. The microbial community composition also shifted accordingly, with a marked increase in the abundance of the *Rummeliibacillus* genus – known for caproate production – at pH 4.5.[19,20] Similarly, Palomo-Briones *et al.* found that pH strongly affected product distribution, with *n*-caproate dominating at pH 5–6 and *n*-caprylate at pH 6.75–7.[21] pH influences osmoregulation, and transmembrane transport,[22] induces changes in the ionisation of substrates or enzymes active sites,[23] interactions between different microorganism groups,[24] shifts in the metabolic pathways, all of which can influence metabolite profile.[24] Furthermore, temperature and HRT may induce substantial changes in the product spectrum and the pathways of active metabolism. Shorter HRTs impose selective pressure on the microbial community, favouring fast-growing fermentative bacteria while increasing the risk of washout of slower-growing species. A reduction in HRT enhances throughput and volumetric productivity[25] and can also alleviate product inhibition.[20] Moreover, decreasing HRT increases the energy transfer efficiency (ε) due to a lower maintenance energy demand,[22] meaning that more energy is directed toward growth and product formation. Temperature, on the other hand, affects enzyme activity and microbial metabolism. An increase in temperature accelerates reaction rates due to the increase in molecular movement rates; however, prolonged exposure to elevated temperatures may lead to enzyme denaturation and a gradual decline or complete cessation of the metabolic activity.[23] Because thermal stability is enzyme and organism-specific,[23] specific temperatures favour particular microbial populations and metabolic pathways, thereby altering both growth rate and the product spectrum. Such temperature-driven metabolic shifts have been reported by Ferreira *et al.*,[26] where mesophilic conditions favoured the aceto-butyric pathway, with higher acetate, butyrate, and H_2 yields, while thermophilic conditions promoted ethanol-type fermentation, with lower H_2 yields. Temperature also affected microbial community composition, with greater diversity in mesophilic conditions. In the same study, HRT strongly influenced hydrogen yields – shortening the HRT from 8 to 4 hours increased the yield by 33%, whereas reducing it to 1 hour, decreased the yield by 62%. The metabolite profile shifted accordingly from lactate, propionate, and caproate at 8 hours HRT to acetate, butyrate, and malate at 1 hour HRT.[26]

This study aimed to evaluate the influence of operational parameters (temperature, pH, HRT) on the production of biochemicals from organic waste streams *via* MCF. Therefore, we screened through key abiotic process parameters, *i.e.*, pH (7.0, 6.5, 6.0, 5.5), temperature (37 °C, 50 °C), and HRT (5.0 days, 2.5 days, 1.25 days) – to determine favourable conditions for the production of target platform chemicals, such as succinate and caproate.

Experimental

Inoculum and influent

The inoculum used in reactors R1 and R2 was an anaerobic sludge, originally sourced from a wastewater treatment plant (Kozieglowy, Poznan area, Poland), that has been maintained and enriched within our research group over several years in various chain elongation studies.[8]

Synthetic OFMSW was prepared with the following composition (w/w): potatoes (22%), apples (20%), carrots (12%), tomatoes (10%), cabbage (7%), bread (6%), rice (5%), pasta

(5%), bananas (5.7%), lemons (5.7%), grass (0.5%), leaves (0.5%), coffee grinds (0.3%) and tea (0.3%). The mixture was mechanically ground using a Thermomix® TM6 (Vorwerk, Germany) at a speed level of 10 for 10 minutes, repeated for two consecutive times. Total Solids (TS), Volatile Solids (VS), and Chemical Oxygen Demand (COD) of the prepared substrate were determined in triplicate, as previously described.[13] The %TS was 15.28 ± 0.01%, of which 96.16 ± 0.01% was VS. The COD of the VS fraction was 133.18 ± 0.01 g L^{-1}. The prepared substrate was stored in aliquots at −20 °C. Before use, it was thawed overnight in a refrigerator and diluted as necessary to achieve a TS content of 4.0%, corresponding to a COD of 34.86 g L^{-1}. The pH measured was 4.29 ± 0.05. The reactors were fed with the substrate at organic loading rates (OLR) of 6.97 g COD per L per day at HRT 5 days, 13.94 g COD per L per day at HRT 2.5 days, and 27.89 g COD per L per day at HRT 1.25 days. To maintain a homogeneous feed and avoid unwanted chemical changes, the substrate was continuously stirred at 350 rpm and kept at 4 °C.

Experimental setup

Two CSTR 1.7 L Lambda Minifor (LAMBDA Laboratory Instruments GmbH, Baar, Switzerland) fermenters with a working volume of 1 L were used. Both R1 and R2 operated as chemostats with automatic monitoring and control of temperature, pH, and agitation. Temperature was maintained by an infrared (IR) radiation heater beneath the fermentation vessel. The pH was adjusted using 4 M sodium hydroxide. Mixing was provided by a fish-tail stirrer set at 2.5 rpm. Substrate was automatically dosed from a refrigerated feed vessel using LeadFluid BT100S (Baoding Lead Fluid Technology Co., Ltd, China) peristaltic. A Ritter MilliGascounter (Ritter, Germany) was used to measure the volume of gases produced during fermentation, and gas samples for GC measurements were collected three times per week. Liquid fermentation broth samples were collected daily, centrifuged at 20 900*g* for 15 min, and stored at −20 °C until further analysis. Details of the downstream processing of the fermentation products are provided in the SI.

Operational phases

Prior to the reactor test runs, the inoculum in R1 was adapted to mesophilic conditions (30 °C, pH 6.5, HRT 5 days), while the inoculum in R2 was adapted to thermophilic conditions and slightly lower pH (50 °C, pH 5.5, HRT 5 days). Both reactors were subsequently operated in continuous mode for 150 days, using the same substrate mixture to enable comparison of temperature effects on product distribution. Reactor operation was divided into seven phases (Table 1).

Analytical techniques

The headspace gas composition (hydrogen, methane, carbon dioxide) was analysed using a gas chromatograph GC-2014 (Shimadzu, Japan) equipped with a thermal conductivity detector (TCD), following the protocol described by Brodowski *et al.*[27] Saccharides, lactic acid, and succinic acid were quantified using a high-performance liquid chromatograph HPLC Prominence (Shimadzu, Japan), following the protocol described by Duber *et al.*[11] Alcohols (ethanol, propanol, isopropanol, butanol, 2-butanol) and carboxylates (acetic acid, butyric acid, iso-butyric acid, valeric acid, iso-valeric acid, caproic acid, iso-caproic acid, enanthic acid, and caprylic acid) were quantified using a GC-2014 (Shimadzu, Japan) equipped with a flame ionization detector (FID), according to the method described by Zagrodnik *et al.*[28] Total Organic Carbon (TOC), Total Inorganic Carbon (TIC), and Total Nitrogen (TN) contents were quantified with a TOC analyzer (Multi N/C 2100s, Analytik Jena, Jena, Germany) using a differential method.[29]

Microbial composition

Microbial composition was analysed using Nanopore sequencing of full-length rRNA operon amplicons. Biomass samples were collected by centrifugation and stored at −20 °C until processing. Genomic DNA was isolated using the ZymoBIOMICS DNA Microprep Kit (ZymoResearch, Poland) according to the manufacturer's recommendations. In the first PCR, amplification of the rrn operon was carried out with Phusion Green Hot Start II High-Fidelity DNA Polymerase (2 U μL^{-1}) and primers 16S-27F (5′-TTTCTGTTGGTGCTGATATTGC AGrGTTTGATyhTGGCTCAG) and 23S-2241R (5′-ACTTGCCTGTCGCTCTATCTTC ACCrCCCCAGThAA-ACT-3′). The resulting amplicons were indexed during 8 cycles in a second PCR reaction, carried out with LongAmp® Hot Start Taq DNA Polymerase (NEB, M0533S), 50 ng of the amplicon, and an individual forward-reverse barcode primer pair for each sample. After pooling barcoded amplicons in equimolar concentration, further library preparation was carried out using Oxford Nanopore Sqk-lsk114 Ligation Kit. Sequencing was done on FLO-MIN114 (R10.4.1) flow cell utilizing MinION Mk1C sequencer

Table 1 A set of phases applied in both reactors during the process

	Inoculum source	Phase I	Phase II	Phase III	Phase IV	Phase V	Phase VI	Phase VII
Days of operation	—	0–35	35–49	49–77	77–96	96–114	114–127	127–150
Reactor 1 (R1)	30 °C, pH 6.5, HRT5	37 °C, pH 6.5, HRT 5	37 °C, pH 5.5, HRT 5	50 °C, pH 5.5, HRT 5	37 °C, pH 6.5, HRT 5	37 °C, pH 7.0, HRT 5	37 °C, pH 7.0, HRT 2.5	37 °C, pH 7.0, HRT 1.25
Reactor 2 (R2)	50 °C, pH 5.5, HRT 5		37 °C, pH 6.0, HRT 5	50 °C, pH 6.0, HRT 5				

(Nanopore Technologies), to the depth of *ca.* 10k full-length amplicons per sample.

Acquired raw data was subsequently basecalled using super-accurate dna_r10.4.1_e8.2_400bps_sup@v4.3.0 model with dorado v0.5.3 basecaller. The reads were run through Duplex Tools v0.2.9[30] to split concatenated reads by Nanopore adapter. Reads were then filtered by average Phred ≥ 10 using NanoFilt v2.8.0[31] and those in size between 3000 bp and 7000 bp were retained for further analysis. Demultiplexing and removal of synthetic sequences were done with a minibar.[32]

Furtheron, reads were classified using the EMU v3.4.1 program by mapping to the rrn operon database, ncbi_202006 "NCBI RRN".[32] A pseudo tax-table containing all samples and phyloseq object was created as described by Petrone *et al.* in https://github.com/josephpetrone/RESCUE.[33] Downstream analyses and visualisations were carried out using the *phyloseq* package.[34] Raw sequences obtained in this study were submitted to the NCBI Sequence Read Archive (SRA) database and are available under BioProject PRJNA1222907.

Statistical and diversity analyses

All statistical analyses were performed on R CRAN software (v4.3.2). The raw counts of sequences, firstly processed using the *phyloseq* package (v1.48.0), were further transformed using the centered log-ratio (CLR) method[35] to address issues of data compositionality. Alpha diversity was assessed to characterize the microbial diversity throughout reactor operation. The Hill diversity numbers were computed using the *vegan* package (v2.6–4), reflecting observed richness, the Shannon, and the inverse Simpson indexes.

Redundancy analysis (RDA) was performed using the *rda()* function from the *vegan* package. The statistically relevant ($p < 0.05$) environmental factors (pH, temperature, and HRT) were used as constraining variables in the analysis, while metabolite concentrations (succinate, caproate, acetate, butyrate, propionate, lactate, and ethanol) were applied as supplementary variables using the *envfit()* function.

Spearman's correlation was conducted in R, using the *cor.test()* function with the method "spearman" to determine the dependencies between concentrations of caproate, ethanol, and lactate.

Calculations

Specificity was calculated as described in ref. 36 using a formula:

$$\text{Specificity}[\%] = \text{product concentration}[\text{mM C}] / \text{sum of all produced carboxylic acids}\,[\text{mM C}] \times 100.$$

Carbon content entering the system (eqn (1)) was determined by TOC (see SI). For the effluent, the total carbon balance (eqn (2)) was calculated as the sum of TOC, TIC, and CO_2 produced:

$$\text{C\_total\_initial} = \text{TOC\_initial} + \text{TIC\_initial} = \text{TC\_initial} \quad (1)$$

$$\text{C\_total\_final} = \text{TOC\_final} + \text{TIC\_final} + \text{CO}_2\text{\_produced} = \text{TC} + \text{CO}_2\text{\_produced} \quad (2)$$

Carbon recovery (eqn (3)) (see SI) was calculated as:

$$\text{Carbon\_recovery}\ (\%) = (\text{C\_total\_final}/\text{C\_total\_initial}) \times 100\%. \quad (3)$$

Results and discussion

pH changes induced metabolic shifts during Phases I and II

In the 35-day Phase I, process parameters were maintained at 37 °C and pH 6.5, and a HRT of 5 days in both reactors. At the start of the process, elevated ethanol concentrations were detected – 415 mM C in R1 and 620 mM C in R2 – carried over from the inoculum. Throughout operation, acetate and butyrate emerged as the main products, reaching concentrations of 172 ± 41 mM C and 158 ± 42 mM C in R1, and 185 ± 82 mM C and 175 ± 53 mM C in R2, respectively (Fig. 1). Caproate and valerate concentrations fluctuated throughout Phase I, with average values of 102 ± 58 mM C and 42 ± 38 mM C in R1, and 39 ± 35 mM C and 23 ± 22 mM C in R2, respectively. Gas production in Phase I was unstable in both reactors (Fig. 2). Only H_2 and CO_2 were detected. On day 7, gas production peaked, reaching 4.8 and 3.0 L day^{-1} of H_2 and CO_2 in R1, and 2.2 and 1.7 L day^{-1} in R2. Thereafter, production rates gradually declined to approximately 0.3 L day^{-1} by day 20 in both reactors.

The peaks in gas formation coincided with an increase in succinate synthesis. Between days 7 and 23, average succinate concentrations were 188 ± 30 mM C in R1 and 155 ± 29 mM C in R2. The maximum values reached 192 mM C in R1 (day 13) and 200 mM C in R2 (day 12). Overall, during days 7–23 of Phase I, succinate was the predominant soluble metabolite, accounting for 28% of the total detected products. According to Kenealy and Waselefsky,[37] when *Clostridium kluyveri* is cultured on ethanol and succinate in the presence of H_2, succinate can be split into two acetate molecules, a reaction that is thermodynamically more favorable than acetate formation from ethanol alone ($\Delta G^{o\prime} \approx -48.6$ kJ *vs.* +9.6 kJ).[37] In our system, ethanol concentrations were initially high and decreased over time, while succinate accumulated and later declined. The early phase, when ethanol was still abundant, together with the detection of *C. kluyveri*–related taxa (Fig. 3), is consistent with possible *C. kluyveri* activity. Subsequently, as ethanol became low or undetectable, the concurrent rise in propionate and decline in succinate suggests a shift toward succinate-to-propionate conversion by propionogenic microorganisms. Between days 13 to 35, the average propionate concentration increased to 153 ± 52 mM C in R1 and 100 ± 48 mM C in R2, with maximum values of 230 and 189 mM C, respectively. These results are consistent with the observations of Yang *et al.*,[38] who reported transient succinate accumulation and subsequent consumption during MCF propionate fermentation conducted at lower pH (<4.5).[38] Similar behaviour was noted by Duber *et al.* in MCF of OFMSW under conditions

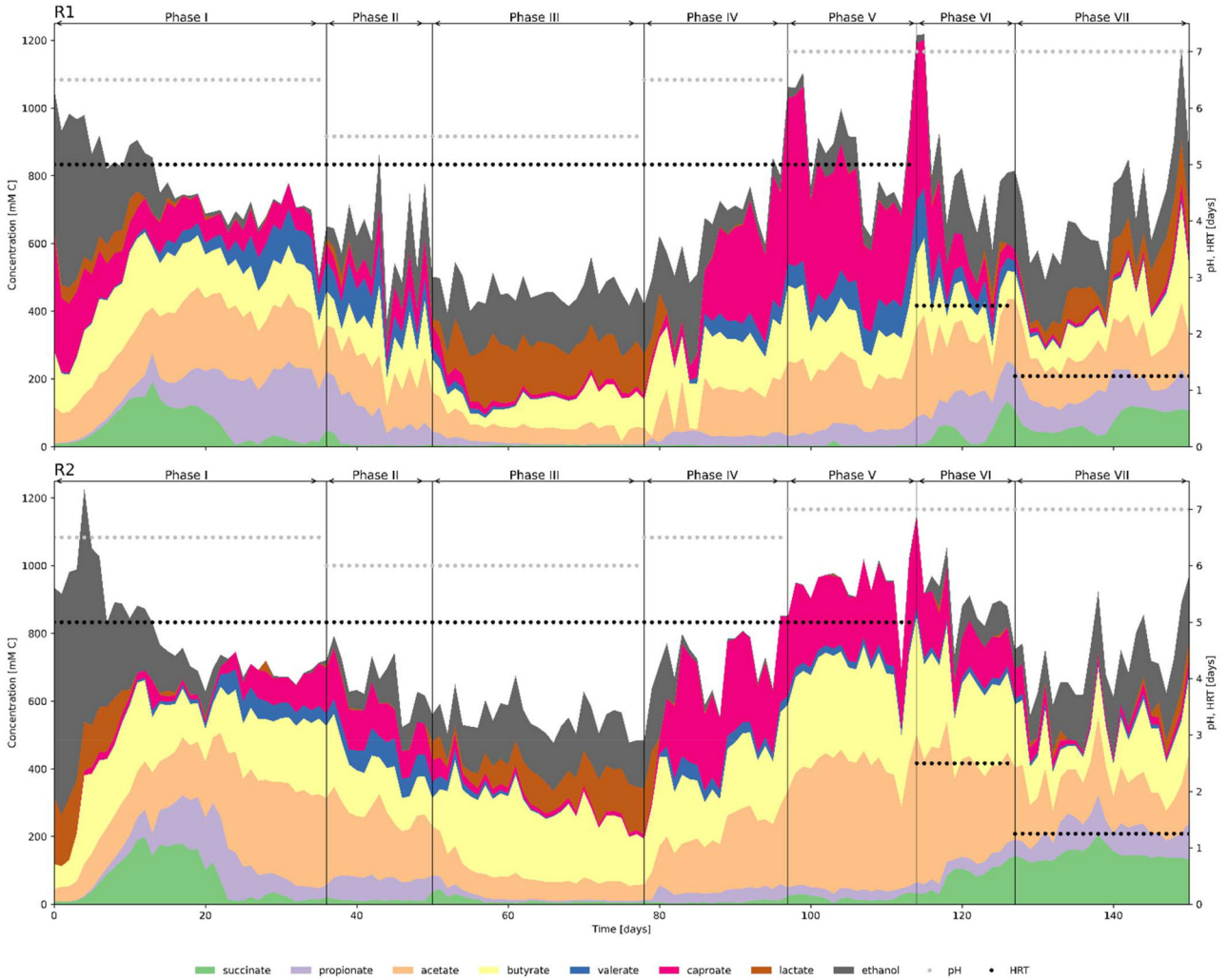

Fig. 1 Cumulative metabolite production profile in R1 and R2. The data represent individual measurements at each sampling point (no replicates). The auxiliary line marked pH and HRT as grey (pH) and black (HRT) points.

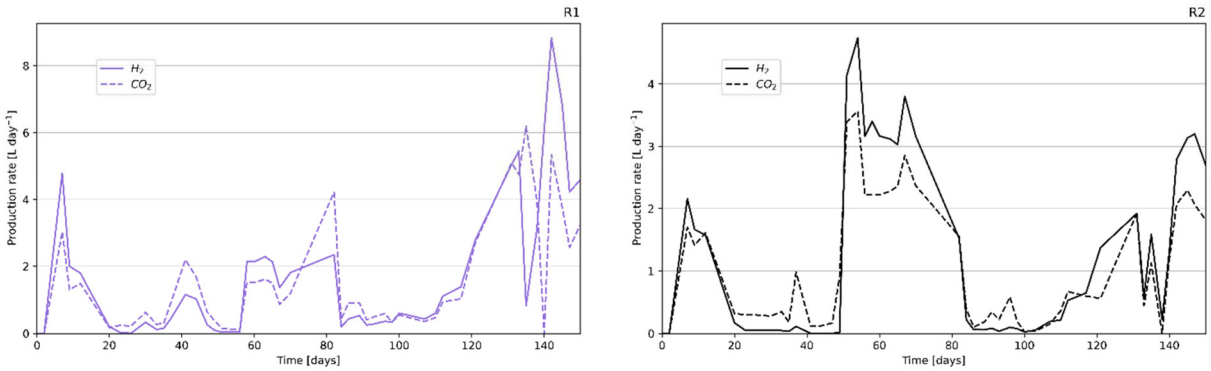

Fig. 2 Gas production rate [L day^{-1}] of H_2 and CO_2 in R1 and R2. Each data point represents a single measurement at the corresponding sampling time.

comparable to our study (37 °C, pH 6.5, and HRT of 5 days), where succinate was produced together with propionate and acetate in approximately 1 : 1 : 1 ratios.[8]

In both R1 and R2, microbial diversity increased during the initial phase and reached a maximum at day 35, with the highest α-diversity observed in R1 (Fig. 4). On day 15, microor-

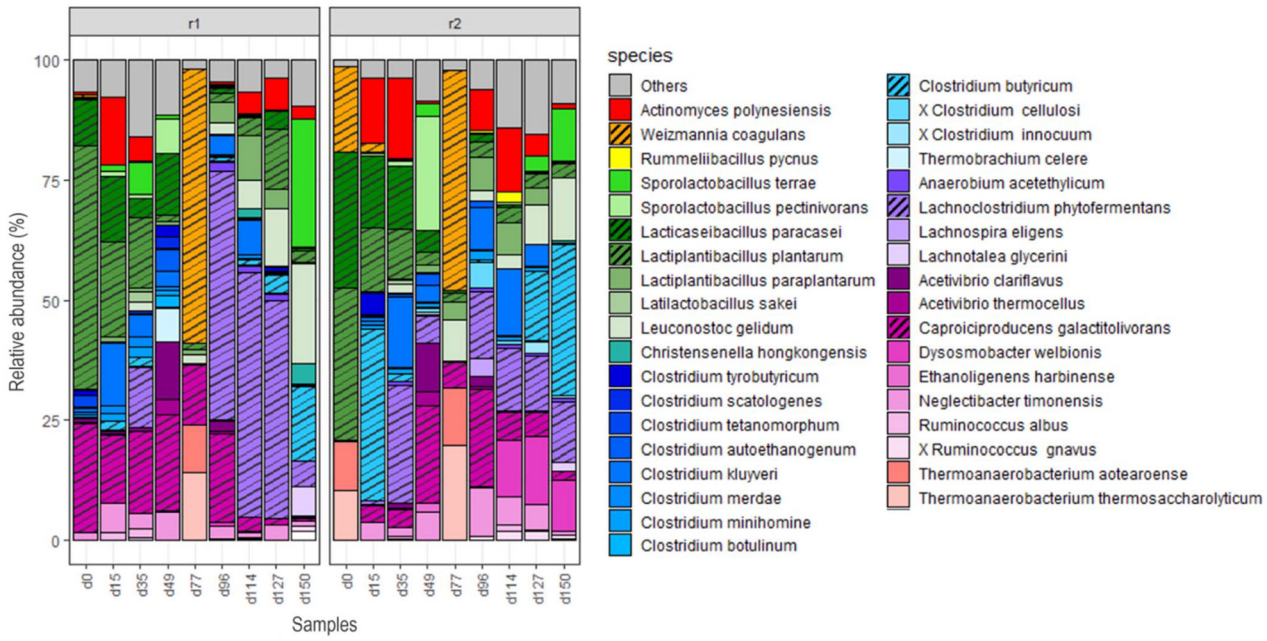

Fig. 3 A bar plot of the reactors' microbiome composition (n = 3) expressed as species-level relative abundances based on total read-mapping counts. For better legibility, average values are displayed without error bars for clear visualisation. Fluctuations are observed in response to the diverse conditions applied. A complementary genus-level heatmap showing relative abundances as percentages is available in the SI for enhanced clarity (Fig. S1).

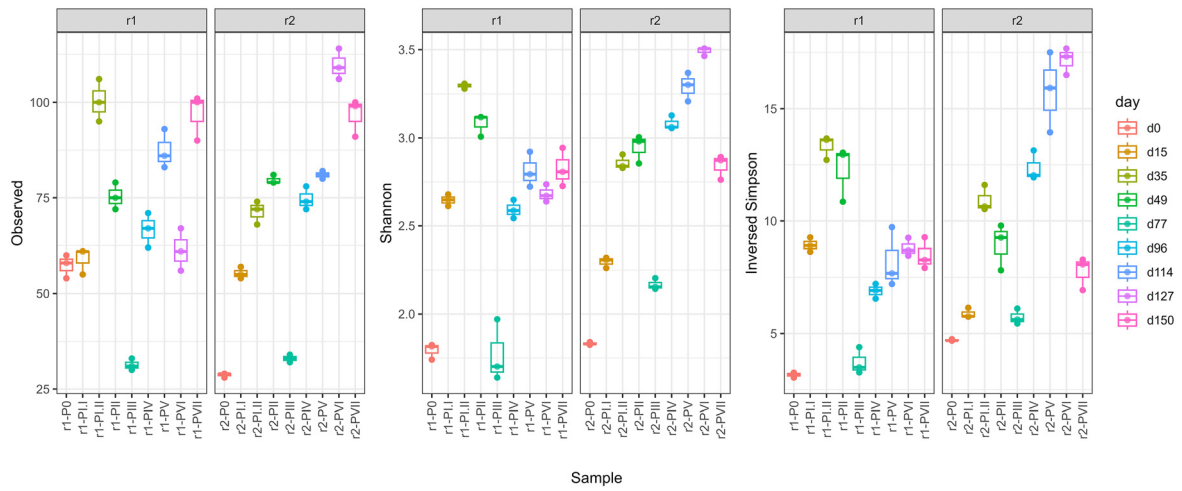

Fig. 4 Reactors' alpha diversity is dependent on the introduced environmental factors. Alpha diversity measures over time for each bioreactor, from left to right: number of observed OTUs, Shannon index, and Inversed Simpson index. Each colour represents a sampling time, and each boxplot summarizes three data points.

ganisms closely related to *C. kluyveri*, *C. butyricum* and *Caproiciproducens galactitolivorans* were detected (Fig. 3). *C. butyricum* is known for butyrate, acetate, propionate, lactate, and succinate production,[39] while *C. galactitolivorans* produces H_2, CO_2, ethanol, acetate, butyrate, and caproate,[40] largely explaining the product profile in Phase I. Additionally, lactic acid bacteria (LAB) affiliated with *Lacticaseibacillus paracasei* and *Lactiplantibacillus plantarum* were detected. Interestingly, Özcelik *et al.*[41] described the ability of LAB to produce succinate and propionate, among other carboxylates. Their temporal co-occurrence during increased succinate and propionate concentrations could suggest a possible association with this metabolism.[41] Additionally, *Actinomyces polynesiensis*-like microorganisms, known to produce lignocellulolytic enzymes,[42] were detected in samples from days 15 and 35. Moreover, cellulolytic bacteria affiliated to *Lachnoclostridium*

phytofermentans[43] emerged in both reactors at day 35, and became the predominant species in R2; their activity can result in the production of ethanol, acetate, CO_2, and H_2.

Guided by the findings of Candry *et al.*,[44] who reported a decrease in propionate production after pH reduction, the pH in Phase II was lowered to 6.0 in R1 and 5.5 in R2. However, in the present study, this adjustment did not lead to a decrease in propionate, nor was any increase in succinate observed. Instead, acetate (144 ± 26 mM C in R1 and 199 ± 37 mM C in R2) and butyrate (116 ± 27 mM C in R1 and 143 ± 37 mM C in R2) emerged as the predominant products. Ethanol (105 ± 43 mM C in R1, 71 ± 34 mM C in R2), propionate (99 ± 46 mM C in R1, 64 ± 10 in R2), caproate (67 ± 23 mM C in R1, 111 ± 22 mM C in R2) and valerate (82 ± 26 mM C in R1, 60 ± 13 mM C in R2) were identified as by-products.

Lowering the pH in Phase II decreased α-diversity (Fig. 4) and re-shaped the microbial community, with Phase II forming a different cluster in the RDA plot (Fig. 5). By day 49,

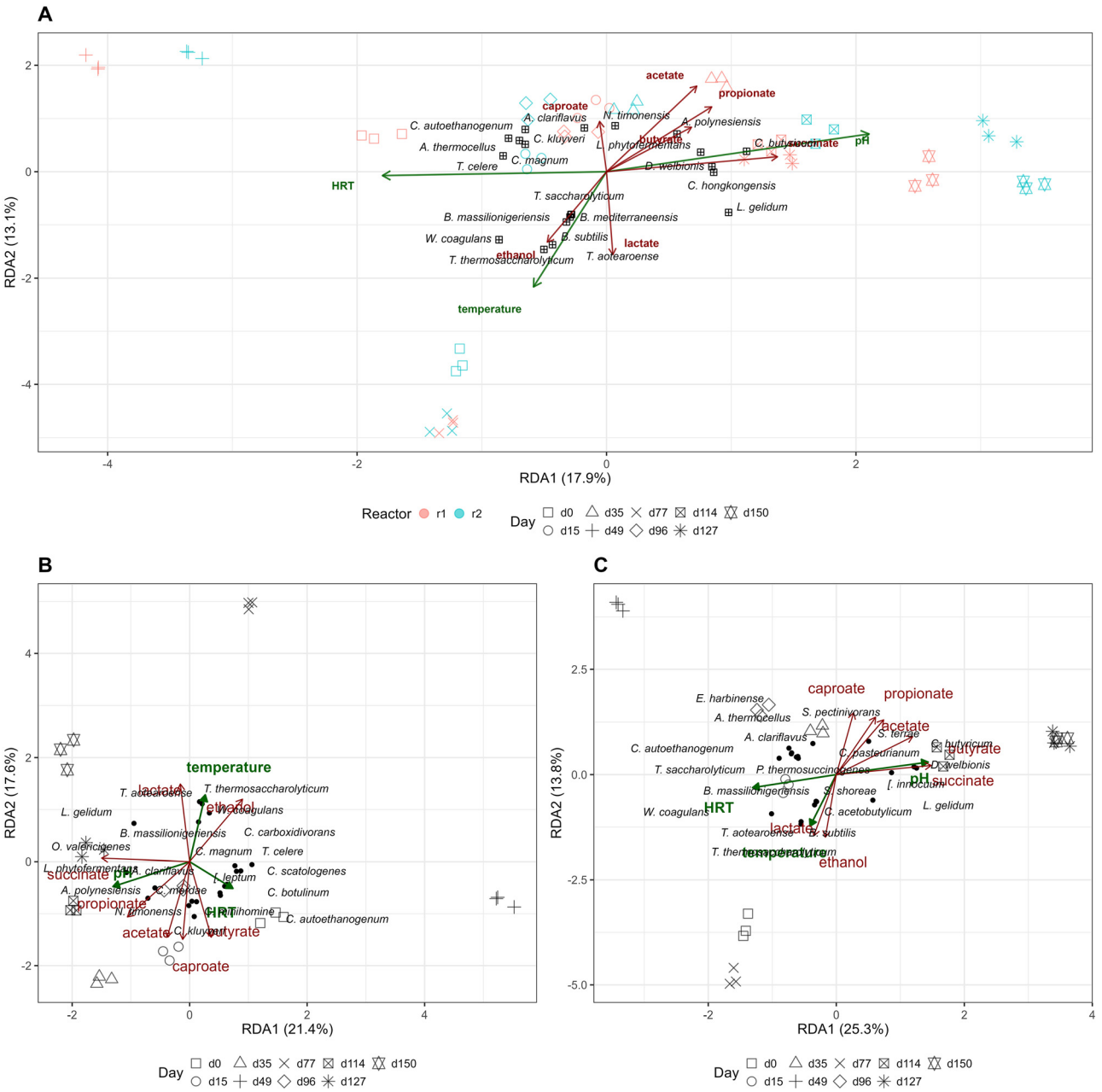

Fig. 5 Redundancy analysis (RDA) plots performed at the OTU-level after CLR normalization of the data. RDA plots for (A) all triplicates, (B) R1 separately, and (C) R2 separately, determine the relationship between the environmental vectors (pH, temperature, and HRT – dark green arrows), the mixed culture composition (black points), and metabolites produced (dark red arrows). The amount of variance explained is indicated on each axis. Each point represents a sample, shaped by the phase.

the microbiomes in both R1 and R2 were characterized by the presence of *C. galactitolivorans*, several *Clostridium* species, members of *Acetivibrio* (cellulolytic acetate producer)[45] and lactic acid bacteria belonging to the genera *Lacticaseibacillus* and *Sporolactobacillus*.[46]

Temperature increase resulted in a decrease in metabolite production during Phase III

Given the findings of Santos *et al.*,[47,48] who observed succinate production using a thermophilic inoculum, we explored whether temperature increase to 50 °C could promote similar activity in the mesophilic communities used in this study. Although succinate concentrations did not increase, the product profile shifted to lactate, ethanol, and butyrate.

During the 28-day Phase III, lactate concentrations increased considerably compared to the previous phase – by approximately 21-fold in R1 (132 ± 36 mM C) and 34-fold in R2 (83 ± 36 mM C). Ethanol levels also rose, by 1.5-fold in R1 and 2-fold in R2, reaching 153 ± 19 mM C and 142 ± 26 mM C, respectively. Butyrate concentrations decreased by 0.7-fold in R1 (to 81 ± 29 mM C), but increased by 1.4-fold in R2 (to 205 ± 43 mM C). Phase III was also the only period associated with a substantial decline in acetate production, with average concentrations of 55 ± 20 mM C in R1 and 69 ± 25 mM C in R2. The concurrent increase in ethanol likely reflects a shift in carbon and electron flow toward more reduced products under thermophilic conditions. Additionally, compared to Phase II, Phase III showed elevated and stable H_2 and CO_2 production, with H_2 production raising by 2.2 fold in R1 (reaching 1.34 ± 0.95 L day^{-1}) and in R2 from negligible amounts to 3.52 ± 0.55 L day^{-1}. CO_2 production in R2 (2.61 ± 0.50 L day^{-1}) was 2.6 times higher than in R1 (0.96 ± 0.62 L day^{-1}).

Overall, Phase III was characterized by lower product yields, reaching only 548 mM C in R1 and 571 mM C in R2, compared to the range of 674–1003 mM C in other phases. Kim *et al.*[49] previously suggested that thermophilic conditions can limit the resources available for metabolite production due to higher decay rates of thermophiles compared to mesophiles. The increased decay rates elevate energy requirements to support cellular maintenance or specific enzyme activity, thereby lowering the efficiency of carbon conversion into metabolites production.[49]

The temperature increase in Phase III reduced the microbiome diversity (Fig. 4), likely due to the thermal denaturation of proteins and enzymes of some mesophiles.[26] At the end of Phase III, only three dominant taxa accounted for approximately 80% of the relative abundance in the microbiomes of both reactors. Sequences affiliated with *Weizmania coagulans*, an α-amylase-secreting, lactate-producing bacterium, represented the largest community fraction. Two taxa assigned to the *Thermoanaerobacterium* genus – whose main fermentation products are ethanol, acetate, lactate (swiftly converted to butyrate), H_2, and CO_2 [50] – constituted the second most abundant group in both reactors during Phase III. These taxa were primarily represented by the cellulose-degrading *Thermoanaerobacterium thermosaccharolyticum*, followed by *Thermoanaerobacterium aotearoense*. Of particular interest, Yang *et al.*[50] reported that under thermophilic conditions, the presence of *T. thermosaccharolyticum* promoted the proliferation of *W. coagulans*. The authors stated that the coexistence of *T. thermosaccharolyticum* and *W. coagulans* decreases the yield of lactate due to its further conversion to butyrate by *T. thermosaccharolyticum*.[50] RDA of R1 and R2 samples in Phase III, illustrated a strong positive association between temperature, the production of ethanol and lactate, and the occurrence of microorganisms closely related to *T. thermosaccharolyticum*, *T. aotearoense*, and *W. coagulans*. The thermophilic phase clustered distinctly in the RDA plot, suggesting a considerably different microbial community composition compared to the mesophilic phases.

Products accumulated during Phase III induced CE in mesophilic Phases IV and V

The product spectrum of Phase III, dominated by lactate, ethanol, and butyrate, created an opportunity to explore the potential for efficient single-stage CE. Hence, in Phase IV, the initial operational conditions – 37 °C and pH 6.5 – were reintroduced in both reactors. After two 5-day HRTs in R1 and one in R2, caproate concentration increased 20.5-fold in R1 (from 12 to 254 mM C) and 18.8-fold in R2 (from 11 to 213 mM C). Other main metabolites were acetate and butyrate, with average concentrations of 182 ± 35 mM C and 155 ± 38 mM C in R1 and 167 ± 39 mM C and 194 ± 39 mM C in R2, respectively. Propionate and valerate were also produced in both reactors, each accounting for approximately 30 mM C. Strikingly, although the same conditions (37 °C, pH 6.5, and HRT 5 days) previously favoured succinate production (in Phase I), in Phase IV succinate appeared only in R2, reaching a maximum concentration of 31 mM C.

A pH increase from 6.5 to 7.0 in Phase V boosted metabolite production in both reactors, resulting in higher total product concentrations – from 660 ± 117 mMC in Phase IV to 968 ± 167 mMC in R1, and from 719 ± 95 mMC to 1003 ± 89 mMC in R2. The higher pH also stimulated caproate formation, leading to a 2.1-fold increase in the caproate production rate (71 ± 17 mM C day^{-1}) in R1, with an average concentration of 355 ± 85 mM C during the 18-day phase and a peak of 515 mM C on day 99. Caproate concentrations also increased in R2, although at a lower rate than in R1. The average caproate production rate in R2 was 48 ± 15 mM C day^{-1}, corresponding to an average concentration of 130 ± 27 mM C. Acetate remained the predominant product in both reactors, averaging 182 ± 35 mM C in R1 and 366 ± 45 mM C in R2. The considerably higher acetate concentrations in the R2, together with nearly undetectable ethanol concentrations, suggest excessive ethanol oxidation to acetate – a well-known competing reaction with CE.[51] This could also potentially explaining lower caproate levels in R2 than in R1. In R1, other fermentation products in Phase V included butyrate (155 ± 38 mM C), valerate (83 ± 24 mM C), and propionate (49 ± 13 mM C). In R2, butyrate was also prominent (289 ± 28 mM C), while valerate (27 ± 4 mM C), propionate (23 ± 3 mM C), and succinate (19 ± 9 mM C) were detected as

by-products. Although the caproate yields were satisfactory, further factors that could enhance production. As recently shown by Wang *et al.*,[52] a more reduced ORP favours the formation of more reduced products, such as caproate.[52] Because ORP was not measured in our study, future work should include ORP monitoring to better elucidate the redox conditions that affect microbial activity and product distribution.

The reenactment of mesophilic conditions with pH increase led to stable gas production throughout Phase IV, with a notable drop in the production of almost all gases (Fig. 2). H_2 decreased to 47% in R1 and 8% in R2 of the levels measured in the previous phase, while CO_2 production rose by 18% in R1 and declined by 81% in R2. Following a pH increase in Phase V, CO_2 further declined by 45% in R1 and 49% in R2, while H_2 levels dropped by 61% in R2, and remained relatively stable in R1. High acetate concentrations combined with low, almost negligible CO_2 amounts suggest a higher activity of the Wood–Ljungdahl pathway.[20]

The change in conditions during Phase IV increased microbial diversity and induced distinct shifts in microbiome composition. *W. coagulans* and *Thermoanaerobacterium* close relatives, which dominated the microbiome in Phase III, were undetectable or nearly undetectable in Phase IV. However, what was observed instead was the co-occurrence of microorganisms closely related to an acetate, ethanol, and H_2-producing *L. phytofermentans* alongside taxa identified as *C. kluyveri* and *C. galactitolivorans*, known caproate producers. Interestingly, *C. galactitolivorans* was the only microorganism present in both Phase III and IV in both reactors. The metabolic activity of *L. phytofermentans* may have supported CE not only due to its cellulolytic abilities,[43] but also by supplying key intermediates – ethanol and H_2 as electron donors, and acetate as the carbon backbone for reverse β-oxidation carried out by *C. kluyveri* and *C. galactitolivorans*. To our knowledge, there is only one study describing *L. phytofermentans* and *C. galactitolivorans* co-occurrence at pH 6.0 and targeting caproate production in MCF; however, in contrast to our results, only acetate and butyrate production were reported, with no increase in caproate levels.[53]

In Phase V, which favoured caproate production, taxa related to *C. galactitolivorans* and *C. kluyveri* were detected in both reactors, possibly supported by lactate-producing bacteria, affiliated with *Lactiplantibacillus paraplantarum* and *A. polynesiensis*. Furthermore, higher caproate concentrations in R2 than in R1 could be explained by a bigger predominance of sequences affiliated with *C. butyricum* and *Dysosmobacter welbionis*, known butyrate producers.

Ethanol drives CE in Phases IV and V

Ethanol, alongside lactate, is a well-known electron donor in reverse β-oxidation (RBO), where acetate serves as the electron acceptor and is converted to butyrate, which can further be elongated to caproate.[54] Although some studies have suggested that the fatty acids biosynthesis (FAB) pathway might also contribute to CE, recent evidence indicates that FAB, being an anabolic pathway, cannot be involved in CE, and it is the RBO instead – supported by TCA-derived metabolites – that plays a predominant role in CE.[55]

Interestingly, periods of elevated caproate concentrations were consistently followed by substantial declines in ethanol levels in both bioreactors (Fig. 6). This trend does not apply to the first 15 days of Phase I, when high ethanol concentration originating from the inoculum was still present. In Phase III, under thermophilic conditions, ethanol concentration in R2 rose steadily, reaching an average of 142 ± 26 mM C, while caproate concentration dropped from 90 mM C (the end of Phase II) to an average concentration of 21 ± 14 mM C. Upon reintroducing mesophilic conditions in Phase IV, ethanol concentrations declined to 49 ± 69 mM C, while caproate increased to 209 ± 92 mM C. Such inverse patterns between ethanol consumption and caproate accumulation have been widely reported in ethanol-driven CE.[56]

To investigate the relationship between ethanol and caproate concentrations, Spearman correlation analysis was performed using data from all triplicates and for each reactor individually. Across all triplicates, a significant negative correlation was observed ($\rho = -0.72$, $p < 0.001$), which was stronger for individual reactors (for R1: $\rho = -0.79$ ($p < 0.001$), and for R2: $\rho = -0.82$ ($p < 0.001$)). The consistent, strong negative correlation between ethanol and caproate, supported by the

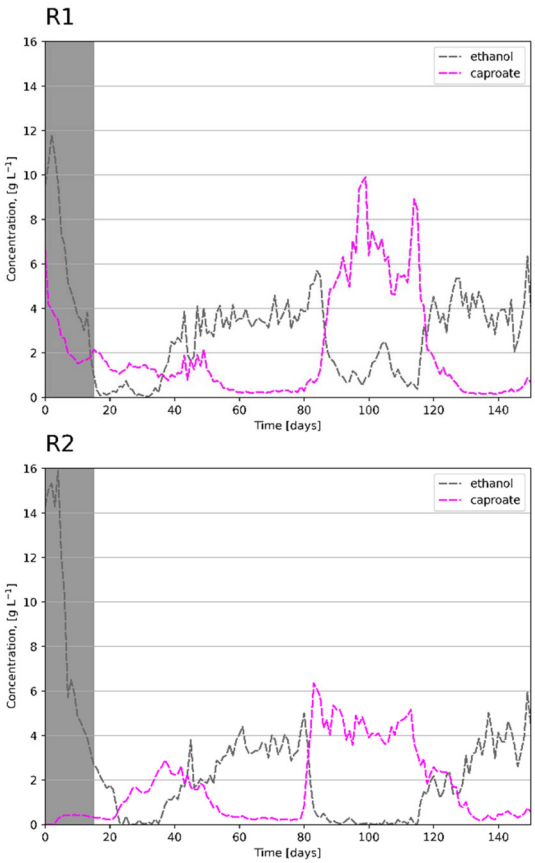

Fig. 6 Caproate-ethanol dependency observed in R1 and R2 (shadowed period shows start-up phase, not representative for dependency).

strong negative correlation in RDA, suggests that ethanol was consumed during caproate production and served as a key substrate in the process. Our findings regarding the influence of ethanol on caproate production align with those reported by others.[8,20,57–59] For instance, in a study by Duber *et al.*,[8] after the pH change from 5.5 to 6.5, ethanol consumption and a three-fold increase in caproate production rate were observed. Moreover, when ethanol was added externally, caproate concentration increased approximately 1.5-fold.[8]

Additionally, Spearman correlation between lactate and caproate was very weak ($\rho = -0.15$, $p = 0.34$ for all triplicates and $\rho = -0.26$, $p = 0.26$ for R1) or moderate ($\rho = -0.41$, $p = 0.07$ for R2). This suggests lactate played a limited role in caproate biosynthesis, with possible reactor-specific effects in R2, reflecting not only differences in substrate availability but also the competitive dynamics of lactate metabolism. The weaker and more variable correlation with lactate in our study indicates it may be less directly involved in caproate biosynthesis or subject to reactor-specific roles, particularly in R2, where the correlation strengthens.[60]

HRT reduction and OLR increase in Phases VI and VII restore succinate production, and eliminate caproate from the product spectrum

In Phase VI, HRT was shortened by half to 2.5 days in both reactors, increasing the OLR from 6.97 to 13.94 g COD per L per day, while maintaining the pH and temperature at 7.0 and 37 °C. The effects differed between the reactors. In R1, the main products were acetate (191 ± 47 mM C), ethanol (150 ± 55 mM C), butyrate (108 ± 41 mM C), and propionate (108 ± 31 mM C), accompanied by a 3.5-fold increase in both CO_2 and H_2 production rates, suggesting a pronounced acidogenic fermentation.[61] In R2, acetate (304 ± 65 mM C) and butyrate (239 ± 31 mM C) predominated, and although CO_2 and H_2 production rates increased 5 and 2-fold, respectively, the effect was less pronounced than in R1. In Phase VII, the HRT was further reduced by half to 1.25 days (OLR = 27.89 g COD per L per day). In R1, ethanol (171 ± 31 mM C), acetate (135 ± 23 mM C), and butyrate (123 ± 55 mM C) were the predominant products, followed by propionate, succinate, and lactate, produced in roughly equal ratios. In R2, the main products were ethanol, succinate, acetate, and butyrate, produced in nearly equal amounts (~147 mM C each). Gas production rates of H_2 and CO_2 in R1 were 2.6 times higher than in R2.

Notably, HRT of 1.25 days, pH 7.0, and 37 °C were the most favorable conditions for succinate production, especially in R2, where relatively stable production (147 ± 19 mM C) was maintained for 23 days with a maximum concentration of 207 mM C. Relative to Phase VI (HRT = 2.5 days), the production rate showed a nearly 3-fold increase to an average of 118 ± 40 mM C day^{-1}. Furthermore, the lower CO_2 production rate in R2 than in R1 during Phases VI and VII, which coincided with higher succinate concentrations, suggests increased CO_2 incorporation into succinate or other TCA-derived intermediates.

R1 was less favorable for succinate production. During Phases I and VI, the propionate production rate in R1 exceeded that of succinate; however, further decrease of the HRT equalized their production rates. Ultimately, after 10 HRTs of 1.25 days, the succinate production rate in R1 surpassed that of propionate. Thus, even though propionate increased in R1 and remained stable in R2 in Phases VI–VII, this did not suppress succinate production as observed in Phase I. These results indicate that shortening the HRT effectively alleviated the suppression of succinate production caused by its conversion to propionate. This claim is supported by the RDA analysis, which illustrates that succinate production has a strong negative correlation with HRT, indicating that lower HRT values are associated with increased succinate production. Additionally, RDA indicates a strong positive correlation with pH, suggesting that maintaining a higher pH further supports succinate synthesis.

Production of succinate in MCF in shorter HRTs was observed also by Fortney *et al.*[62] and Ferreira *et al.*[63] Approximately 3-fold increase in succinate concentration (from 2 to 5–6 g COD per L) was observed by Fortney *et al.*[62] in mesophilic thin stillage MCF when SRT (Solids Retention Time), which in that case was equal to HRT, was shortened from 6 to 1 day.[62] In turn, in dark fermentation of cane molasses conducted by Ferreira *et al.*[63] succinate was the predominant product in mesophilic conditions at HRT of 8 hours, consisting of 81.4% of all products produced. Thus, both studies support the hypothesis that shorter HRTs may enhance succinate production in MCF. However, in the Ferreira *et al.*[63] study, by shortening HRT to as short as one hour, metabolism shifted towards H_2 production, and succinate was no longer produced,[63] highlighting the threshold below which HRT becomes unfavorable for succinate synthesis.

The effect of HRT shortening in Phase VI on caproate production was unclear. In R1, caproate production rate decreased by 33% (to 48 ± 39 mM C day^{-1}), and concentration decreased 3-fold to 121 ± 110 mM C, whereas in R2, the average production rate increased by 13% (to 55 ± 16 mM C day^{-1}) while concentrations decreased 2-fold to 130 ± 27 mM C. The more rapid decrease in caproate levels may be attributed to the differences in microbiome composition between R1 and R2, with an increased fraction of caproate producers (close relatives of *C. galactitolivorans* and *C. kluyveri*). As at HRT 2.5 days, the peak of caproate production rate was observed in R2; the results are consistent with Bian *et al.*,[64] who reported optimal production under similar conditions (35 °C and pH 5.5–6.0, 2.5-day HRT) with *Megasphaera* and *Caproiciproducens* identified as the key chain-elongating microbes.[64]

Given that shorter HRT can favor faster-growing microorganisms and induce the wash-out of slower-growing microbes,[65] throughout Phases VI and VII, the R1 and R2 microbiome composition fluctuated (Fig. 3). Overall, the observed α-diversity increased in both reactors between Phases V (HRT 5 days) and VII (HRT 1.25 days), induced by shortening HRT. However, in Phase VI, after reduction of HRT to 2.5 days, the effect on α-diversity was reactor-specific – the decrease was observed in R1, and an increase in R2. With the decline in HRT, the fraction of sequences assigned as *Leuconostoc*

gelidum and *Sporolactobacillus terrae*, *L. plantarum*, known lactate producers,[66,67] was more pronounced in both reactors. As lactate levels were low in both reactors in Phase VI (2–10 mM C), and Phase VII in R2 (16 ± 19 mM C), and increased only in R1 in Phase VII (78 ± 41 mM C), this suggests it could have been transformed into other compounds. The RDA analysis associates *L. gelidum* in R1 with succinate and lactate, and in R2 with succinate; and *S. terrae* in R2 with acetate and propionate. Likewise, *C. butyricum* close relative, was detected in both Phases VI and VII. In fact, RDA points to *C. butyricum* and *D. welbionis* as associated with succinate and butyrate production in R2. The correlation regarding *C. butyricum* is in line with the study by Oka *et al.*,[39] reporting that *C. butyricum* produces butyrate and succinate, among other products (acetate, ethanol, lactate, propionate, H_2).[39]

Summary and conclusions

Current global and societal challenges have been the main driving force in exploring new avenues for sustainable chemical production: (i) the need to defossilise the chemical industry while preserving biomass for food and feed; and (ii) the accumulation of organic waste. In this context, anaerobic MCF was investigated as a strategy for carbon recovery through the production of added-value biochemicals. The objectives of this study were to produce succinate and medium-chain carboxylates (mainly caproate), among others, from organic waste and to determine the most favourable operational conditions for their synthesis.

The results show how the operational parameters shaped the product spectrum, microbial composition, and α-diversity in MCF. Most importantly, shortening the HRT expanded the product spectrum and increased overall production rates in both reactors, including higher succinate concentrations. The most favourable conditions for stable succinate production were pH 7.0, 37 °C, and HRT of 1.25, achieving a substantial productivity of 118 ± 40 mM C (3.43 g L^{-1} day^{-1}). In contrast, thermophilic conditions decreased metabolite productivity and narrowed the product spectrum to lactate, ethanol, and butyrate, thus creating a basis for CE. Under mesophilic conditions (both at pH 6.5 and pH 7.0, and HRT of 5 days), significant caproate production was observed, reaching a maximum concentration of 515 mM C at neutral pH.

While these results are promising for expanding the product spectrum achievable in mixed cultures, it is acknowledged that, for succinate in particular, both the titer and overall yield remain lower than those typically reported for pure culture fermentations.[68] For future implementation, several environmental and process aspects should be considered.[69] The development of microbial consortia capable of operating at lower pH could substantially reduce reagent consumption in fermentation,[70] thereby improving both economic and environmental performance, especially since NaOH requirements are the main environmental impact drivers of the fermentation process.[71] A direct utilization of low-value, unprocessed waste feedstocks, with the elimination of sterilisation requirements[11–13] reduces upstream energy inputs and capital and operating costs compared to pure culture fermentation, demonstrating a key advantage of mixed cultures – their potential to reduce environmental burdens associated with chemical production. Additionally, mixed cultures eliminate the need for enzymatic hydrolysis of complex substrates, which decreases the upstream costs compared to pure culture fermentation.[72] The separation of carboxylic acids has been identified as a major cost driver in bioprocessing,[69,72] accounting for 43–62% of total succinic acid industrial production costs,[69] highlighting the importance of developing efficient recovery strategies. A detailed comparison of energy consumption and current efficiency for electrodialysis with bipolar membrane (EDBM) separation across different studies is provided in SI Table S2. Recent studies have established economic and environmental benchmarks for bio-based organic acid production. Ioannidou *et al.* (2023) evaluated OFMSW biorefineries against conventional waste management practices and found GHG savings of 0.95–2.06 kg CO_2-eq per kg dry OFMSW processed.[71] Moreover, the study stressed that integrating the developed processes with biofertilizer and biogas production from residual biorefinery solids would further improve overall process sustainability.[71]

Future work should include a techno-economic analysis (TEA) or life-cycle assessment (LCA) specific to our system to evaluate both economic viability and environmental sustainability. Moreover, future research should focus on a deeper investigation of microbial interactions and thermodynamic constraints within MCF systems to enhance process understanding, control, and optimization. These advancements will be essential to achieving higher product titres and yields, and ultimately, to render the process industrially viable.

Author contributions

Conceptualization: H. P., P. O. P.; data curation: H. P., E. A., M. L.; formal analysis: H. P., M. S., E. A., M. L.; funding acquisition: P. O. P.; investigation: H. P., M. S., N. G.; methodology: H. P., M. S., N. G., E. A., M. L., P. O. P.; project administration: P. O. P.; resources: H. P., M. S., N. G., N. Y. W., M. L., P. O. P.; supervision: M. L., P. O. P.; visualization: H. P., E. A., M. L.; writing – original draft: H. P.; writing – review & editing: H. P., M. S., N. G., E. A., N. Y. W., M. L., D. Z. S., P. O. P.

Conflicts of interest

There are no conflicts to declare.

Data availability

The supporting data has been provided as part of the Supplementary information. See DOI: https://doi.org/10.1039/d5gc05638a.

Acknowledgements

This work was financed by the National Science Center, Poland, under grant agreement no. UMO-2021/43/B/ST8/00393. The graphical abstract, and Fig. S2 were created with BioRender.com. The authors thank Joanna Chwiałkowska for conducting the TOC analysis.

References

1 A. van der Linden and A. Reichel, Bio-waste in Europe—turning challenges into opportunities, https://www.eea.europa.eu/publications/bio-waste-in-europe, (accessed November 19, 2024).
2 R. Moscoviz, E. Trably, N. Bernet and H. Carrère, *Green Chem.*, 2018, **20**, 3159–3179.
3 Municipal waste statistics, https://ec.europa.eu/eurostat/statistics-explained/index.php?title=Municipal_waste_statistics, (accessed November 21, 2024).
4 Glossary, https://ec.europa.eu/eurostat/statistics-explained/index.php?title=Glossary:Municipal_waste, (accessed November 20, 2024).
5 D. P. Ghumra, O. Rathi, T. A. Mule, V. S. Khadye, A. Chavan, F. C. Barba, S. Main, A. Odaneth and B. N. Thorat, *Biofuels, Bioprod. Biorefin.*, 2022, **16**, 877–890.
6 O. US EPA, Wastes, https://www.epa.gov/report-environment/wastes, (accessed November 20, 2024).
7 A. P. Gupte, N. Di Vita, M. W. Myburgh, R. A. Cripwell, M. Basaglia, W. H. van Zyl, M. Viljoen-Bloom, S. Casella and L. Favaro, *Energy Convers. Manage.*, 2024, **302**, 118105.
8 A. Duber, R. Zagrodnik, N. Gutowska, F. Brodowski, T. Dąbrowski, S. Dąbrowski, M. Łężyk and P. Oleskowicz-Popiel, *Bioresour. Technol.*, 2025, 131697.
9 C. Zerfaß, J. Chen and O. S. Soyer, *Curr. Opin. Biotechnol.*, 2018, **50**, 121–127.
10 B. Colombo, F. Favini, B. Scaglia, T. P. Sciarria, G. D'Imporzano, M. Pognani, A. Alekseeva, G. Eisele, C. Cosentino and F. Adani, *Biotechnol. Biofuels*, 2017, **10**, 201.
11 A. Duber, L. Jaroszynski, R. Zagrodnik, J. Chwialkowska, W. Juzwa, S. Ciesielski and P. Oleskowicz-Popiel, *Green Chem.*, 2018, **20**, 3790–3803.
12 P. Candry and R. Ganigué, *Curr. Opin. Biotechnol.*, 2021, **67**, 99–110.
13 E. Jankowska, J. Chwiałkowska, M. Stodolny and P. Oleskowicz-Popiel, *Bioresour. Technol.*, 2015, **190**, 274–280.
14 S. Giri, S. Waschina, C. Kaleta and C. Kost, *J. Mol. Biol.*, 2019, **431**, 4712–4731.
15 M. J. Scarborough, C. E. Lawson, A. C. DeCola and I. M. Gois, *Curr. Opin. Microbiol.*, 2022, **65**, 8–14.
16 S. Ben Said, R. Tecon, B. Borer and D. Or, *Curr. Opin. Biotechnol.*, 2020, **62**, 137–145.
17 S. Louca, M. F. Polz, F. Mazel, M. B. N. Albright, J. A. Huber, M. I. O'Connor, M. Ackermann, A. S. Hahn, D. S. Srivastava, S. A. Crowe, M. Doebeli and L. W. Parfrey, *Nat. Ecol. Evol.*, 2018, **2**, 936–943.
18 X. Yang, K. Feng, S. Wang, M. M. Yuan, X. Peng, Q. He, D. Wang, W. Shen, B. Zhao, X. Du, Y. Wang, L. Wang, D. Cao, W. Liu, J. Wang and Y. Deng, *Microbiome*, 2024, **12**, 166.
19 C. Quintela, A. Grimalt-Alemany, O. Modin, Y. Nygård, L. Olsson, I. V. Skiadas and H. N. Gavala, *Biomass Bioenergy*, 2024, **187**, 107292.
20 W. Dong, Y. Yang, C. Liu, J. Zhang, J. Pan, L. Luo, G. Wu, M. K. Awasthi and B. Yan, *Renewable Sustainable Energy Rev.*, 2023, **175**, 113181.
21 R. Palomo-Briones, J. Xu, C. M. Spirito, J. G. Usack, L. H. Trondsen, J. J. L. Guzman and L. T. Angenent, *Chem. Eng. J.*, 2022, **446**, 137170.
22 J.-R. Bastidas-Oyanedel, C.-A. Aceves-Lara, G. Ruiz-Filippi and J.-P. Steyer, *Eng. Life Sci.*, 2008, **8**, 487–498.
23 P. K. Robinson, *Essays Biochem.*, 2015, **59**, 1–41.
24 Z. E. Ilhan, A. K. Marcus, D.-W. Kang, B. E. Rittmann and R. Krajmalnik-Brown, *mSphere*, 2017, **2**, e00047–17.
25 V. De Groof, M. Coma, T. Arnot, D. J. Leak and A. B. Lanham, *Waste Manage.*, 2021, **127**, 80–89.
26 T. B. Ferreira, G. C. Rego, L. R. Ramos, L. A. Soares, I. K. Sakamoto, L. L. de Oliveira, M. B. A. Varesche and E. L. Silva, *Int. J. Hydrogen Energy*, 2018, **43**, 18908–18917.
27 F. Brodowski, M. Łężyk, N. Gutowska and P. Oleskowicz-Popiel, *Sci. Total Environ.*, 2022, **802**, 149885.
28 R. Zagrodnik, A. Duber, M. Łężyk and P. Oleskowicz-Popiel, *Environ. Sci. Technol.*, 2020, **54**, 5864–5873.
29 J. Buchholz, M. Graf, B. Blombach and R. Takors, *Biochem. Eng. J.*, 2014, **90**, 162–169.
30 Nanoporetech/duplex-tools Oxford Nanopore Technologies 2024.
31 W. De Coster, S. D'Hert, D. T. Schultz, M. Cruts and C. Van Broeckhoven, *Bioinformatics*, 2018, **34**, 2666–2669.
32 H. Krehenwinkel, A. Pomerantz, J. B. Henderson, S. R. Kennedy, J. Y. Lim, V. Swamy, J. D. Shoobridge, N. Graham, N. H. Patel, R. G. Gillespie and S. Prost, *GigaScience*, 2019, **8**, giz006.
33 Petroovius, josephpetrone/RESCUEhttps://github.com/josephpetrone/RESCUE 2024.
34 P. J. McMurdie and S. Holmes, *PLoS One*, 2013, **8**, e61217.
35 G. B. Gloor, J. M. Macklaim, V. Pawlowsky-Glahn and J. J. Egozcue, *Front. Microbiol.*, 2017, **8**, 2224.
36 Y. Zhang, X. Pan, J. Zuo and J. Hu, *Bioresour. Technol.*, 2022, **343**, 126144.
37 W. R. Kenealy and D. M. Waselefsky, *Arch. Microbiol.*, 1985, **141**, 187–194.
38 Y. Yang, C. Liu, W. Zhao, M. Mazarji, L. Ren, C. Liu, J. Pan and B. Yan, *Chem. Eng. J.*, 2024, **486**, 150190.
39 K. Oka, E. McCartney, T. Ariyoshi, H. Kudo, B. Vilá, L. de Jong, K. Kozłowski, J. Jankowski, S. Morgan, C. Kruger and M. Takahashi, *Toxicol. Res. Appl.*, 2019, **3**, 2397847319826955.
40 B.-C. Kim, B. S. Jeon, S. Kim, H. Kim, Y. Um and B.-I. Sang, *Int. J. Syst. Evol. Microbiol.*, 2015, **65**, 4902–4908.

41 S. Özcelik, E. Kuley and F. Özogul, *LWT*, 2016, **73**, 536–542.
42 A. Saini, N. K. Aggarwal, A. Sharma and A. Yadav, *Enzyme Res.*, 2015, **2015**, 279381.
43 T. A. Warnick, B. A. Methé and S. B. Leschine, *Int. J. Syst. Evol. Microbiol.*, 2002, **52**, 1155–1160.
44 P. Candry, L. Radić, J. Favere, J. M. Carvajal-Arroyo, K. Rabaey and R. Ganigué, *Water Res.*, 2020, **186**, 116396.
45 K. Šuchová and V. Puchart, *Appl. Microbiol. Biotechnol.*, 2025, **109**, 105.
46 X. Guo, L. Yu, M. Xiao, X. Zang, C. Zhang, A. Narbad, W. Chen, F. Tian and Q. Zhai, *Curr. Res. Food Sci.*, 2024, **9**, 100822.
47 S. C. Santos, P. R. F. Rosa, I. K. Sakamoto, M. B. A. Varesche and E. L. Silva, *Int. J. Hydrogen Energy*, 2014, **39**, 9599–9610.
48 S. C. Santos, P. R. F. Rosa, I. K. Sakamoto, M. B. A. Varesche and E. L. Silva, *Int. J. Hydrogen Energy*, 2014, **39**, 9000–9011.
49 M. Kim, Y.-H. Ahn and R. E. Speece, *Water Res.*, 2002, **36**, 4369–4385.
50 L. Yang, L. Chen, H. Li, Z. Deng and J. Liu, *J. Environ. Manage.*, 2022, **304**, 114312.
51 C. Quintela, E. Peshkepia, A. Grimalt-Alemany, Y. Nygård, L. Olsson, I. V. Skiadas and H. N. Gavala, *Waste Biomass Valorization*, 2024, **15**, 2545–2558.
52 Y. Wang, W. Wei, S.-L. Wu and B.-J. Ni, *Environ. Sci. Technol.*, 2020, **54**, 10904–10915.
53 D.-K. Qian, Z.-Q. Geng, T. Sun, K. Dai, W. Zhang, R. J. Zeng and F. Zhang, *Bioresour. Technol.*, 2020, **308**, 123318.
54 C. Fernández-Blanco, A. Pereira, M. C. Veiga, C. Kennes and R. Ganigué, *Bioresour. Technol.*, 2024, **408**, 131138.
55 K. Gemeinhardt, B. S. Jeon, J. N. Ntihuga, H. Wang, C. Schlaiß, T. N. Lucas, I. Bessarab, N. Nalpas, N. Zhou, J. Usack, D. H. Huson, R. Williams, B. Macek, L. Aristilde and L. T. Angenent, *Green Chem.*, 2025, **27**, 2931.
56 M. Roghair, T. Hoogstad, D. P. B. T. B. Strik, C. M. Plugge, P. H. A. Timmers, R. A. Weusthuis, M. E. Bruins and C. J. N. Buisman, *Environ. Sci. Technol.*, 2018, **52**, 1496–1505.
57 M. Roghair, Y. Liu, D. P. B. T. B. Strik, R. A. Weusthuis, M. E. Bruins and C. J. N. Buisman, *Front. Bioeng. Biotechnol.*, 2018, **6**, 7499–7506.
58 W. Huo, X. Fu, M. Bao, R. Ye, Y. Shao, Y. Liu, J. Bi, X. Shi and W. Lu, *Sci. Total Environ.*, 2022, **846**, 157492.
59 C. Zhang, Z. Ling, L. Yang, Y. Liu, T. Cao, Y. Sun, W. Liu, S. Huo, Z.-H. Zhang, H. Su, J. Baeyens and X. Qi, *J. Cleaner Prod.*, 2023, **383**, 135394.
60 F. Brodowski, N. Gutowska, A. Duber, R. Zagrodnik, M. Łężyk and P. Oleskowicz-Popiel, *Chem. Eng. J.*, 2025, **519**, 165367.
61 O. Sarkar, S. K. Butti and S. V. Mohan, in *Waste Biorefinery*, ed. T. Bhaskar, A. Pandey, S. V. Mohan, D.-J. Lee and S. K. Khanal, Elsevier, 2018, pp. 203–218.
62 N. W. Fortney, N. J. Hanson, P. R. F. Rosa, T. J. Donohue and D. R. Noguera, *Front. Bioeng. Biotechnol.*, 2021, **9**, 696306.
63 T. B. Ferreira, G. C. Rego, L. R. Ramos, C. A. de Menezes and E. L. Silva, *Int. J. Energy Res.*, 2020, **44**, 10442–10452.
64 B. Bian, W. Zhang, N. Yu, W. Yang, J. Xu, B. E. Logan and P. E. Saikaly, *Environ. Sci. Ecotechnology*, 2024, **21**, 100424.
65 X. Zhu, X. Feng, C. Liang, J. Li, J. Jia, L. Feng, Y. Tao and Y. Chen, *Appl. Environ. Microbiol.*, 2021, **87**, e03075–20.
66 P. Johansson, E. Säde, J. Hultman, P. Auvinen and J. Björkroth, *BMC Genomics*, 2022, **23**, 818.
67 K. Huang, J. Ni, K. Xu, H. Tang, F. Tao and P. Xu, *Genome Announc.*, 2014, **2**, e00465–14.
68 S. Das, K. Sharma, D. Sharmmah, S. Sharma, S. Sevda and A. A. Prabhu, *Biotechnol. Sustain. Mater.*, 2024, **1**, 15.
69 R. Dickson, E. Mancini, N. Garg, J. M. Woodley, K. V. Gernaey, M. Pinelo, J. Liu and S. S. Mansouri, *Energy Environ. Sci.*, 2021, **14**, 3542–3558.
70 M. L. Jansen and W. M. van Gulik, *Curr. Opin. Biotechnol.*, 2014, **30**, 190–197.
71 S.-M. Ioannidou, J. P. López-Gómez, J. Venus, M. A. Valera, V. Eßmann, I. Alegria-Dallo, I. K. Kookos, A. Koutinas and D. Ladakis, *Green Chem.*, 2023, **25**, 4482–4500.
72 D. Ladakis, E. Stylianou, S.-M. Ioannidou, A. Koutinas and C. Pateraki, *Bioresour. Technol.*, 2022, **354**, 127172.